A Non-homogeneous Time Mixed Integer LP Formulation for Traffic Signal Control

Iain Guilliard
National ICT Australia
7 London Circuit
Canberra, ACT, Australia
iguilliard@nicta.com.au

Scott Sanner
Oregon State University
1148 Kelley Engineering Center
Corvallis, OR 97331
scott.sanner@oregonstate.edu

Felipe W. Trevizan
National ICT Australia
7 London Circuit
Canberra, ACT, Australia
felipe.trevizan@nicta.com.au

Brian C. Williams
Massachusetts Institute of Technology
77 Massachusetts Avenue
Cambridge, MA 02139
williams@csail.mit.edu

ABSTRACT

We build on the body of work in mixed integer linear programming (MILP) approaches that attempt to jointly optimize traffic signal control over an *entire traffic network* (rather than focus on arterial routes) and specifically on improving the scalability of these methods for large urban traffic networks. Our primary insight in this work stems from the fact that MILP-based approaches to traffic control used in a receding horizon control manner (that replan at fixed time intervals) need to compute high fidelity control policies only for the early stages of the signal plan; therefore, coarser time steps can be employed to "see" over a long horizon to preemptively adapt to distant platoons and other predicted long-term changes in traffic flows. To this end, we contribute the queue transmission model (QTM) which blends elements of cell-based and link-based modeling approaches to enable a non-homogeneous MILP formulation of traffic signal control. We then experiment with this novel QTM-based MILP control in a range of networks demonstrating the improved scalability possible with non-homogeneous time steps in comparison to the best homogeneous time step. Our experiments also provide near-optimal traffic control policies for larger horizons and larger networks than shown in previous implementations of MILP-based traffic signal control.

Using 204 words up to here. Maximum is 250 words.

[1]

---

[1]Make sure to follow instructions and author guide: http://onlinepubs.trb.org/onlinepubs/AM/InfoForAuthors.pdf http://onlinepubs.trb.org/onlinepubs/am/2015/WritingForTheTRRecord.pdf

Also note this example related paper from Steve Smith (formatted to TRB specs): https://www.ri.cmu.edu/pub_files/2014/1/TRB14UTC.pdf

1 INTRODUCTION

2 As cities rapidly grow in population while urban traffic infrastructure often adapts at a slower pace,
3 it is critical to maximize capacity and throughput of existing road infrastructure through optimized
4 traffic signal control. Unfortunately, many large cities still use some degree of *fixed-time* control
5 (e.g., Toronto (*1*)) even if they also use *actuated* or *adaptive* control methods such as SCATS (*2*)
6 or SCOOT (*3*). However, there is further opportunity to improve traffic signal control even beyond
7 adaptive methods through the use of *optimized* controllers as evidenced in a variety of approaches
8 ranging from mixed integer (linear) programming (*4, 5, 6, 7, 8, 9*) to heuristic search (*10, 11*) to
9 scheduling (*12*) to reinforcement learning (*1*). While such optimized controllers hold the promise
10 of maximizing existing infrastructure capacity by finding more complex (and potentially closer to
11 optimal) jointly coordinated intersection policies than arterially-focused master-slave approaches
12 such as SCATS and SCOOT, such optimized methods are computationally demanding and either
13 (a) do not guarantee jointly optimal solutions over a large intersection network (often because they
14 only consider coordination of neighboring intersections or arterial routes) or (b) fail to scale to
15 large intersection networks simply for computational reasons (which is the case for many mixed
16 integer programming approaches).

17   In this work, we build on the body of work in mixed integer linear programming (MILP) ap-
18 proaches that attempt to jointly optimize traffic signal control over an *entire traffic network* (rather
19 than focus on arterial routes) and specifically on improving the scalability of these methods for
20 large urban traffic networks. In our investigation of existing approaches in this vein, namely exem-
21 plar methods in the spirit of (*6, 8, 9*) that use a (modified) cell transmission model (CTM) (*13, 14*)
22 for their underlying prediction of traffic flows, we remark that a major drawback is the CTM-
23 imposed requirement to choose a predetermined homogeneous (and often necessarily small) time
24 step for reasonable modeling fidelity. This need to model large number of CTM cells with a small
25 time step leads to MILPs that are exceedingly large and intractable to solve.

26   Our primary insight in this work stems from the fact that MILP-based approaches to traffic
27 control used in a receding horizon control manner (that replan at fixed time intervals) need to
28 compute high fidelity control policies only for the early stages of the signal plan; therefore, coarser
29 time steps can be employed to "see" over a long horizon to preemptively adapt to distant platoons
30 and other predicted long-term changes in traffic flows. This need for non-homogeneous control
31 in turn spawns the need for an additional innovation: we require a traffic flow model that permits
32 non-homogeneous time steps and properly models the travel time delay between lights. To this
33 end, we might consider CTM extensions such as the variable cell length CTM (*15*), stochastic
34 CTM extensions (*16, 17*), extensions for better modeling freeway-urban interactions (*18*) including
35 CTM hybrids with link-based models (*19*), assymmetric CTMs for better handling flow imbalances
36 in merging roads (*20*), the situational CTM for better modeling of boundary conditions (*21*), and
37 the lagged CTM for improved modeling of the flow density relation (*22*). However, despite the
38 widespread varieties of the CTM and the usage of the CTM (*23*) for a range of applications, there
39 seems to be no extension that permits non-homogeneous time steps as required in our novel MILP-
40 based control approach.

41   For this reason, as a major contribution of this work to enable our non-homogeneous
42 time MILP-based model of joint intersection control, we contribute the queue transmission model
43 (QTM) which blends elements of cell-based and link-based modeling approaches with the follow-
44 ing key benefits:

1 • unlike previous joint intersection control work (*6, 8, 9*), it is inherently intended for *non-*
2 *homogeneous* time steps that can be used for control over large horizons,

3 • any length of roadway with no merges or diverges can be modeled as a single queue
4 leading to compact models of large traffic networks thus maintaining relatively compact
5 MILPs for large traffic networks (i.e., larges numbers of cells are not required between
6 intersections), and

7 • it accurately models fixed travel time delays critical to green wave coordination as in (*4,*
8 *5, 7*) through the use of a non-first order Markovian update model and combines this with
9 the more global intersection signal optimization approach of (*6, 8, 9*).

10 In the remainder of this paper, we first formalize our novel QTM model of traffic flow
11 with non-homogeneous time steps and show how to encode it as a linear program for simulating
12 traffic. We proceed to allow the traffic signals to become discrete variables subject to a delay
13 minimizing optimization objective and standard cycle and phase time constraints leading to our
14 final MILP formulation of traffic signal control. We then experiment with this novel QTM-based
15 MILP control in a range of networks demonstrating the improved scalability possible with non-
16 homogeneous time steps in comparison to the best homogeneous time step. These experiments also
17 provide near-optimal traffic control policies for larger horizons and larger networks than shown in
18 previous implementations of MILP-based traffic signal control. [2] [3]

19 **THE QUEUE TRANSMISSION MODEL**
20 A Queue Transmission Model (QTM) is the tuple $(\mathcal{Q}, \mathcal{L}, \vec{\Delta t}, \mathbf{I})$, where $\mathcal{Q}$ and $\mathcal{L}$ are, respectively,
21 the set of queues and lights; $\vec{\Delta t}$ is a vector of size N representing the discretization of the simulation
22 horizon $[0, \mathrm{T}]$ and the duration in seconds of the n-th time interval is denoted as Δt_n; and $\mathbf{I}$ is a
23 matrix $|\mathcal{Q}| \times \mathrm{T}$ in which $I_{i,n}$ represents the flow of cars requesting to enter queue i from the outside
24 of the network at time n.
25 A **traffic light** $\ell \in \mathcal{L}$ is defined as the tuple $(\Psi_\ell^{\min}, \Psi_\ell^{\max}, \mathcal{P}_\ell, \vec{\Phi}_\ell^{\min}, \vec{\Phi}_\ell^{\max})$, where:

26 • $\mathcal{P}_\ell$ is the set of phases of ℓ;

27 • $\Psi_\ell^{\min}$ ($\Psi_\ell^{\max}$) is the minimum (maximum) allowed cycle time for ℓ; and

28 • $\vec{\Phi}_\ell^{\min}$ ($\vec{\Phi}_\ell^{\max}$) is a vector of size $|\mathcal{P}_\ell|$ and $\Phi_{\ell,k}^{\min}$ ($\Phi_{\ell,k}^{\max}$) is the minimum (maximum) allowed
29 time for phase $k \in \mathcal{P}_\ell$.

30 A **queue** $i \in \mathcal{Q}$ represents a segment of road that vehicles traverse at free flow speed; once
31 traversed, the vehicles are vertically stacked in a stop line queue. Formally, a queue i is defined by
32 the tuple $(\mathrm{Q}_i, \mathrm{T}_i^{\mathrm{prop}}, \mathrm{F}_i^{\mathrm{out}}, \vec{F}_i, \vec{Pr}_i, \mathcal{Q}_i^{\mathcal{P}})$ where:

---

[2] We could really use some pictures in the Intro to refer to here and subsequently – both a traffic network divided into queues, and the concept of the piecewise linear evolution of traffic flow with **non-homogeneous** (dilated) time steps, something like I had provided in my early writeup. I think these help visually explain much of the context for the paper and its approach and are critical for reviewer understanding on a time budget for reading this They may only read the first 2-3 pages and then skim!

[3] A picture is worth a 1000 words but we only pay 250, hence a 4X ROI on pictures!

1   • Q_i is the maximum capacity of i;

2   • T_i^{prop} is the time required to traverse i and reach the stop line;

3   • F_i^{out} represents the maximum traffic flow from i to the outside of the modeled network;

4   • $\vec{F}_i$ and $\vec{Pr}_i$ are vectors of size $|\mathcal{Q}|$ and their j-th entry (i.e., $F_{i,j}$ and $Pr_{i,j}$) represent the
5   maximum flow from queue i to j and the turn probability from i to j ($\sum_{j \in \mathcal{Q}} Pr_{i,j} = 1$),
6   respectively; and

7   • $\mathcal{Q}_i^{\mathcal{P}}$ denotes the set of traffic light phases controlling the outflow of queue i.

8   Differently than CTM (8, 13), QTM does not assume that $\Delta t_n = T_i^{\text{prop}}$ for all $n \in \{1, \ldots, N\}$,
9   that is, the QTM can represent non-homogeneous time intervals. The only requirement over Δt_n is
10   that no traffic light maximum phase time is smaller than any Δt_n since phase changes occur only
11   between time intervals; formally, $\Delta t_n \leq \min_{\ell \in \mathcal{L}, k \in \mathcal{P}_\ell} \Phi_{\ell,k}^{\max}$ for all $n \in \{1, \ldots, N\}$. [4]

Traffic Flow Simulation with QTM

13   In this section, we present how to simulate traffic flow in a network using QTM and non-homogeneous
14   time intervals Δt. We assume for the remainder of this section that a *valid* control plan for
15   all traffic lights is fixed and given as parameter; formally, for all $\ell \in \mathcal{L}$, $k \in \mathcal{P}_\ell$, and interval
16   $n \in \{1, \ldots, N\}$, the binary variable $p_{\ell,k,n}$ is known a priori and indicates if phase k of light ℓ is
17   active (i.e., $p_{\ell,k,n} = 1$) or not on interval n.
18   We represent the problem of finding the flow between queues as a Linear Program (LP)
19   over the following variables defined for all interval $n \in \{1, \ldots, N\}$ and queues i and j:

20   • $q_{i,n} \in [0, Q_i]$: traffic volume waiting in the stop line of queue i at the beginning of
21   interval n;

22   • $f_{i,n}^{\text{in}} \in [0, I_{i,n}]$: inflow to the network via queue i during interval n;

23   • $f_{i,n}^{\text{out}} \in [0, F_i^{\text{out}}]$: outflow from the network via queue i during interval n; and

24   • $f_{i,j,n} \in [0, F_{i,j}]$: flow from queue i into queue j during interval n.

25   The maximum traffic flow from queue i to queue j is enforced by constraints (C1) and (C2).
26   (C1) ensures that only the fraction $Pr_{i,j}$ of the total internal outflow of i goes to j, and (C2) forces
27   the flow from i to j to be zero if all phases controlling i are inactive (i.e., $p_{\ell,k,n} = 0$ for all $k \in \mathcal{Q}_i^{\mathcal{P}}$).
28   If more than one phase $p_{\ell,k,n}$ is active, then (C2) is subsumed by the domain upper bound of $f_{i,j,n}$.

$$f_{i,j,n} \leq Pr_{i,j} \sum_{k=1}^{|\mathcal{Q}|} f_{i,k,n} \tag{C1}$$

$$f_{i,j,n} \leq F_{i,j} \sum_{p_{\ell,k,n} \in \mathcal{Q}_i^{\mathcal{P}}} p_{\ell,k,n} \tag{C2}$$

---

[4]**To Iain**: Maybe bring forward a small network and any other figure that would help illustrate the model and comment about it.

1   To simplify the presentation of remainder of the LP, we define the helper variables $q_{i,n}^{\text{in}}$ (C3),
2   $q_{i,n}^{\text{out}}$ (C4), and t_n (C5) to represent the volume of traffic to enter and leave queue i during interval n,
3   and the time elapsed since the beginning of the simulation until the end of interval Δt_n.

$$q_{i,n}^{\text{in}} = \Delta t_n \left(f_{i,n}^{\text{in}} + \sum_{j=1}^{|\mathcal{Q}|} f_{j,i,n} \right) \tag{C3}$$

$$q_{i,n}^{\text{out}} = \Delta t_n \left(f_{i,n}^{\text{out}} + \sum_{j=1}^{|\mathcal{Q}|} f_{i,j,n} \right) \tag{C4}$$

$$t_n = \sum_{x=1}^{n} \Delta t_x \tag{C5}$$

8   In order to account for the misalignment of the different Δt and $\mathrm{T}_i^{\text{prop}}$, we need to find the
9   volume of traffic that entered queue i between two arbitrary points in time x and y ($x \in [0, \mathrm{T}], y \in$
10   $[0, \mathrm{T}]$, and $x < y$), i.e., x and y might not coincide with any t_n for $n \in \{1, \dots, N\}$. This volume
11   of traffic, denoted as $V_i(x, y)$, is obtained by integrating $q_{i,n}^{\text{in}}$ over $[x, y]$ and is defined in (1) where
12   m and w are the index of the time intervals s.t. $t_m \le x < t_{m+1}$, and $t_w \le y < t_{w+1}$. Because
13   the QTM dynamics is piecewise linear, $q_{i,n}^{\text{in}}$ is a step function w.r.t. time and this integral reduces
14   to the sum of $q_{i,n}^{\text{in}}$ over the intervals contained in $[x, y]$ and the appropriate fraction of $q_{i,m}^{\text{in}}$ and $q_{i,w}^{\text{in}}$
15   representing the misaligned beginning and end of $[x, y]$.

$$V_i(x, y) = (t_{m+1} - x) \frac{q_{i,m}^{\text{in}}}{\Delta t_m} + \sum_{k=m+1}^{w-1} q_{i,k}^{\text{in}} + (y - t_w) \frac{q_{i,w}^{\text{in}}}{\Delta t_w} \tag{1}$$

17   Using these helper variables, (C6) represents the flow conservation principle for queue i
18   where $V_i(t_{n-1} - \mathrm{T}_i^{\text{prop}}, t_n - \mathrm{T}_i^{\text{prop}})$ is the volume of cars that reached stop line during Δt_n. Since
19   $\vec{\Delta} t$ and $\mathrm{T}_i^{\text{prop}}$ for all queues are known a priori, the indexes m and w used by V_i can be pre-
20   computed in order to encode (1); moreover, (C6) represents a non-first order Markovian update
21   because the update considers the previous $w - m$ time steps. To insure that the total volume of
22   traffic traversing i (i.e., $V_i(t_n - \mathrm{T}_i^{\text{prop}}, t_n)$) and waiting at the stop line does not exceed the capacity
23   of the queue, we apply (C7).

$$q_{i,n} = q_{i,n-1} - q_{i,n-1}^{\text{out}} + V_i(t_{n-1} - \mathrm{T}_i^{\text{prop}}, t_n - \mathrm{T}_i^{\text{prop}}) \tag{C6}$$

$$V_i(t_n - \mathrm{T}_i^{\text{prop}}, t_n) + q_{i,n} \le \mathrm{Q}_i \tag{C7}$$

27   As with MILP formulations of CTM (e.g. Lin and Wang (8)), QTM is also susceptible to
28   *withholding traffic*, i.e., the optimizer might prevent cars from moving from i to j even though
29   the associated traffic phase is active and j is not full. We address this issue through our objective
30   function (O1) by maximizing the total outflow $q_{i,n}^{\text{out}}$ (i.e., both internal and external outflow) of i
31   plus the inflow $f_{i,n}^{\text{in}}$ from the outside of the network to i. This quantity is weighted by the remaining
32   time until the end of the simulation horizon T to force the optimizer to allow as much traffic volume
33   as possible into the network and move traffic to the outside the network as soon as possible. (O1)
34   is analogous to minimizing delay in CTM models, e.g., (O1) is equivalent to the objective function

(a)

(b)

(c)

(d)
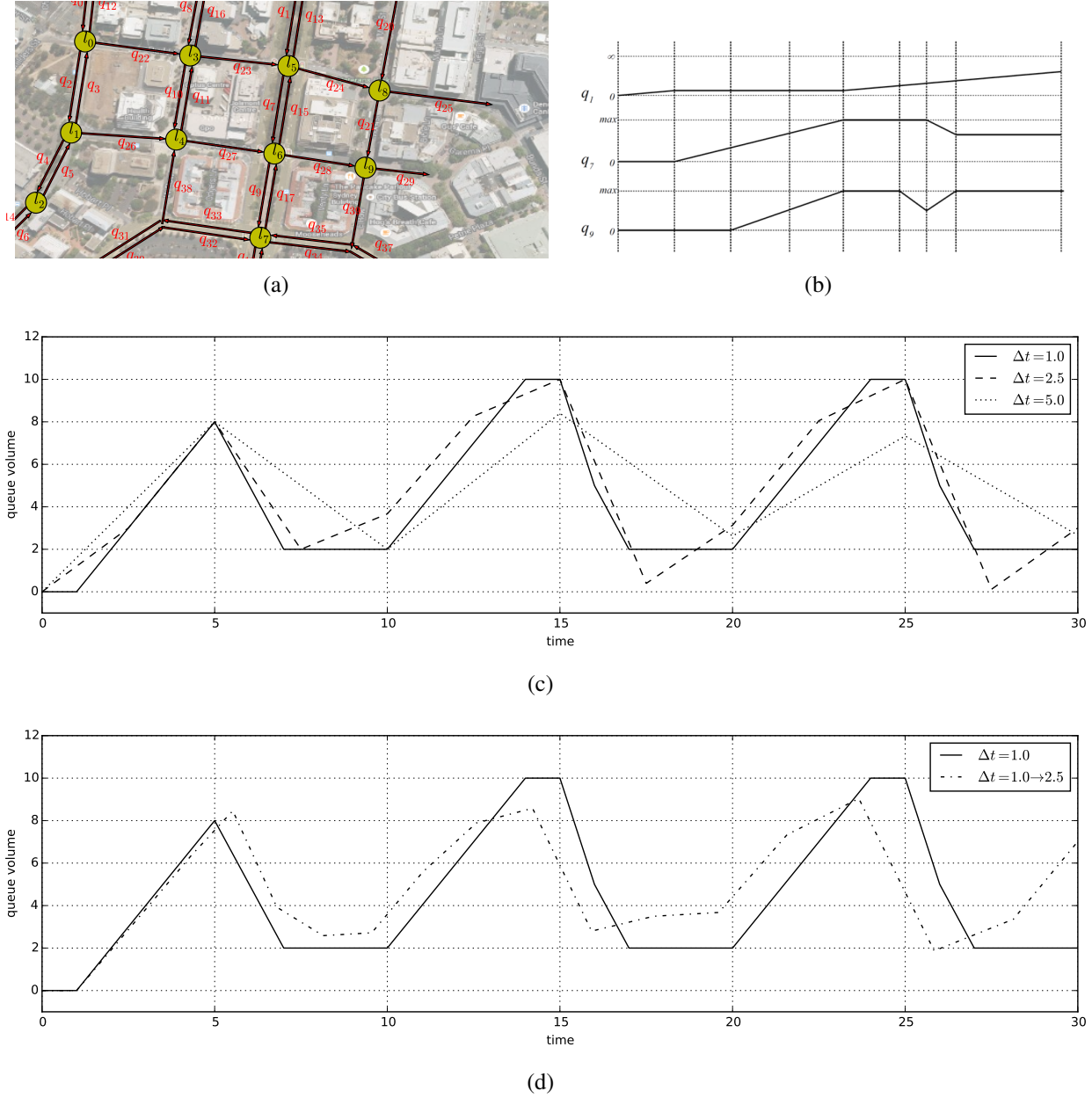
FIGURE 1 A QTM example showing the evolution of traffic volume in q_{27} over time. (a) Streetmap overlay showing how each queue in QTM network corresponds to a segment of roadway and each light to a controlled intersection. (b) Convergence with increasing refinement of Δt from 5.0 down to 1.0. (c) Dilation of Δt from 1.0 to 2.5 compared to a fixed Δt of 1.0.

1 (O3) in Lin and Wang (8) for their parameters $\alpha = \beta = 1$. [5] Figure 3 shows the delay experienced
2 by each vehicle travelling through a network, where delay is the horizontal difference at each point
3 between the cumulative departure and arrival curves, less the free flow travel time through the
4 network. The objective function tries to maximise the depature curve by pushing it up closer to the

---

[5]**To Iain**: Add a paragraph linking the plots with the objective function.
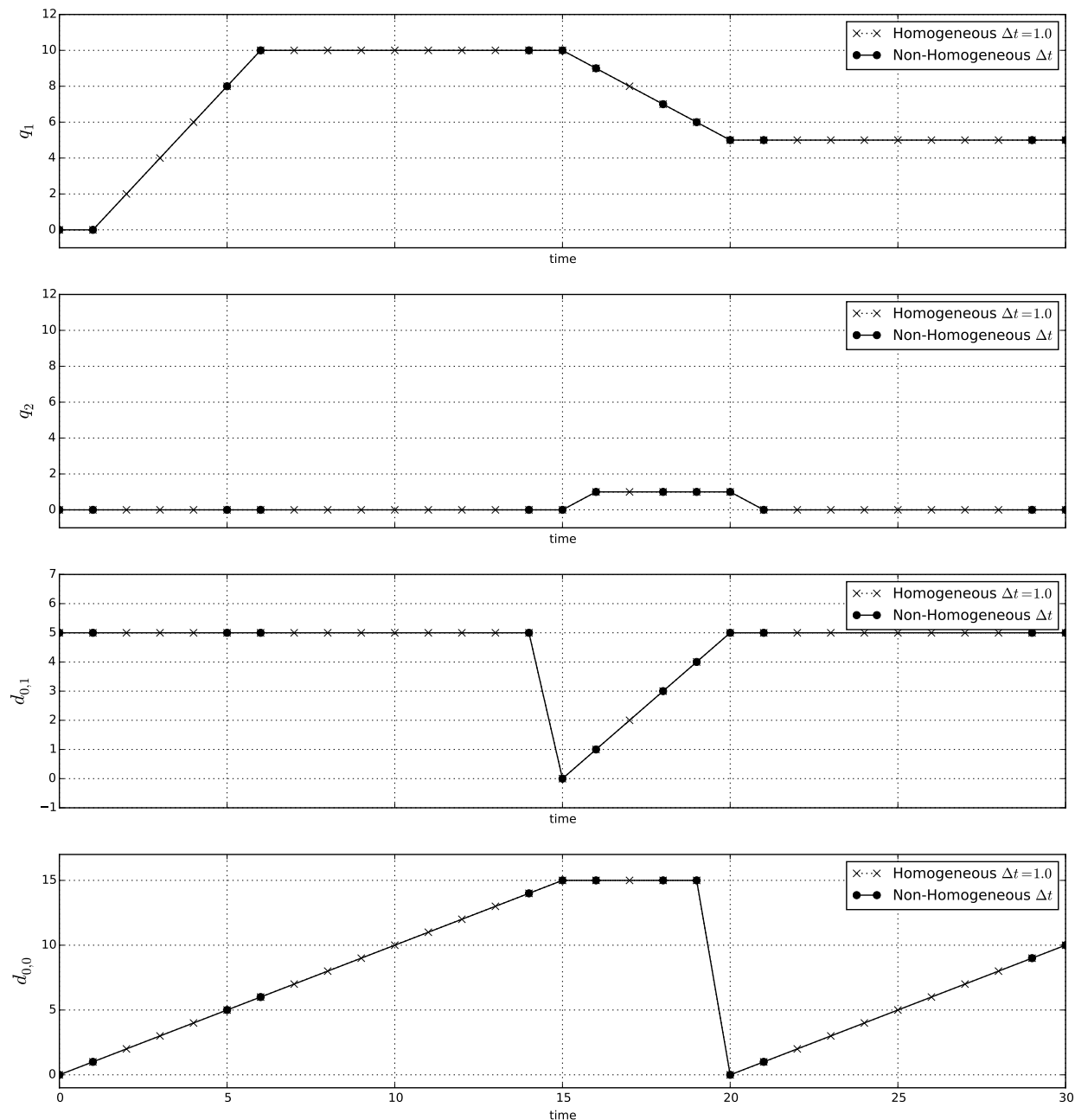
FIGURE 2 An example showing the convergence between a homogeneous solution with $\Delta t = 1.0$ and a non-homogeneous solution over 30 seconds for the same network. By using non-homogeneous time steps the same solution is found with only 14 sample points compared to 30 for homogeneous solution.

1   departure curve, which also has the effect of minimising the horizontal distance, or delay. [6]

---

[6]Show diagrams with traffic predictions converging as time increment gets smaller. Validates that large time-steps are rough approximations while model behavior converges for small time steps.
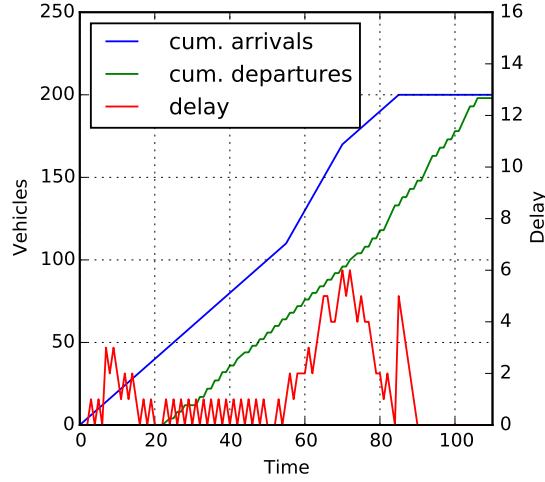
FIGURE 3 **Cumulative arrival (blue) and departure (green) curves, and the resulting delay curve (red). The departure curve is maximized by the objective function, which has the same effect as minimizing the delay curve**

$$\max \sum_{n=1}^{N} \sum_{i=1}^{|\mathcal{Q}|} (T - t_n + 1)(q_{i,n}^{\text{out}} + f_{i,n}^{\text{in}}) \tag{O1}$$

The objective function (O1) and constraints (C1–C7) form the LP representing the dynamic, piecewise linear model of flow in a QTM network over time when a control plan $p_{\ell,k,n}$ is given as an input parameter.

Figures 1(c), 1(d) and 2 show the results of applying the LP formulation to a simple model with a fixed signal plan, using both homogeneous $\vec{\Delta t}$ and non-homogeneous $\vec{\Delta t}$.

TRAFFIC CONTROL WITH QTM AS AN MILP

In this section, we remove the assumption that a valid control plan for all traffic lights is given and extend the LP (O1, C1–C7) to an Mixed-Integer LP (MILP) that also computes the optimal control plan. Formally, for all $\ell \in \mathcal{L}$, $k \in \mathcal{P}_\ell$, and interval $n \in \{1, \ldots, N\}$, the phase activation parameter $p_{\ell,k,n} \in \{0,1\}$ becomes a free variable to be optimized. In order to obtain a valid control plan, we enforce that one phase of traffic light ℓ is always active at any interval n (C8) and that phase changes happen sequentially (C9), i.e., if phase k was active during interval $n-1$ and has become inactive in interval n, then phase $k+1$ must be active in interval n. (C9) assumes that $k+1$ equals 1 if $k = |\mathcal{P}_\ell|$. [7]

$$\sum_{k=1}^{|\mathcal{P}_\ell|} p_{\ell,k,n} = 1 \tag{C8}$$

$$p_{\ell,k,n-1} \leq p_{\ell,k,n} + p_{\ell,k+1,n} \tag{C9}$$

---

[7]**To Iain**: I removed the constraint $p_{\ell,k,n} + p_{\ell,k+1,n} \leq 1$ because it is subsumed by $p_{\ell,k,n} \in \{0,1\}$ and (C8)

1   Next, we enforce the minimum and maximum phase durations (i.e., $\Phi_{\ell,k}^{\min}$ and $\Phi_{\ell,k}^{\max}$) for
2   each phase $k \in \mathcal{P}_\ell$ of traffic light ℓ. To encode these constraints, we use the helper variable
3    $d_{\ell,k,n} \in [0, \Phi_{\ell,k}^{\max}]$ defined by constraints (C10–C14) that: (i) holds the elapsed time since the start
4   of phase k when $p_{\ell,k,n}$ is active (C10,C11) (Figure 4(a)); (ii) is constant and holds the duration of
5   the last phase until the next activation when $p_{\ell,k,n}$ is inactive (C12,C13) (Figure 4(b)); and (iii) is
6   restarted when phase k changes from inactive to active (C14) (Figure 4(c)). Notice that (C10–C14)
7   employs the *big-M* method to turn the cases that should not be active into subsumed constraints
8   based on the value of $p_{\ell,k,}$. We use $\Phi_{\ell,k}^{\max}$ as our large constant since $d_{\ell,k,n} \leq \Phi_{\ell,k}^{\max}$ and $\Delta t_n \leq \Phi_{\ell,k}^{\max}$
9   by assumption (Section 2.1). Similarly, constraint (C15) ensures the minimum phase time of k and
10   is not enforced while k is still active.

11
$$d_{\ell,k,n} \leq d_{\ell,k,n-1} + \Delta t_{n-1} p_{\ell,k,n-1} + \Phi_{\ell,k}^{\max}(1 - p_{\ell,k,n-1}) \tag{C10}$$

12
$$d_{\ell,k,n} \geq d_{\ell,k,n-1} + \Delta t_{n-1} p_{\ell,k,n-1} - \Phi_{\ell,k}^{\max}(1 - p_{\ell,k,n-1}) \tag{C11}$$

13
$$d_{\ell,k,n} \leq d_{\ell,k,n-1} + \Phi_{\ell,k}^{\max} p_{\ell,k,n-1}{}^{8} \tag{C12}$$

14
$$d_{\ell,k,n} \geq d_{\ell,k,n-1} - \Phi_{\ell,k}^{\max} p_{\ell,k,n} \tag{C13}$$

15
$$d_{\ell,k,n} \leq \Phi_{\ell,k}^{\max}(1 - p_{\ell,k,n} + p_{\ell,k,n-1}) \tag{C14}$$

16
17
$$d_{\ell,k,n} \geq \Phi_{\ell,k}^{\min}(1 - p_{\ell,k,n}) \tag{C15}$$

18   Finally, we constrain the sum of all the phase durations for light ℓ to be within the cycle
19   time limits $\Psi_\ell^{\min}$ (C16) and $\Psi_\ell^{\max}$ (C17) (Figure 4(d)). In both (C16) and (C17), we use the duration
20   of phase 1 of ℓ from the previous interval $n - 1$ instead of the current interval n because (C14)
21   forces $d_{\ell,1,n}$ to be 0 at the beginning of each cycle; however, from the previous end of phase 1 until
22   $n - 1$, $d_{\ell,1,n-1}$ holds the correct elapse time of phase 1. Additionally, (C16) is enforced right after
23   the end of the each cycle, i.e., when its first phase is changed from inactive to active. [9]

24
$$d_{\ell,1,n-1} + \sum_{k=2}^{|\mathcal{P}_\ell|} d_{\ell,k,n} \geq \Psi_\ell^{\min}(p_{k,1,n} - p_{k,1,n-1}) \tag{C16}$$

25
$$d_{\ell,1,n-1} + \sum_{k=2}^{|\mathcal{P}_\ell|} d_{\ell,k,n} \leq \Psi_\ell^{\max} \tag{C17}$$

26

27   The MILP that encodes the problem of finding the optimal traffic control plan in a QTM network
28   is defined by (O1, C1–C17).

29   **EMPIRICAL EVALUATION**
30   In this section we compare the solutions for traffic networks modeled as a QTM using homoge-
31   neous and non-homogeneous time intervals in two aspects: the quality of the solution and con-
32   vergence to the optimal solution.[10] We compare the quality of solutions based on the total travel
33   time and we also consider the third quartile and maximum of the observed delay distribution. Our
34   hypotheses are: (i) the quality of the non-homogeneous solutions is at least as good as the homoge-
35   neous ones when the number of time intervals N is fixed; and (ii) the non-homogeneous approach

---

[9]**To Iain**: Relate the phase and cycle constraints with the plots
[10]FWT: I don't think that optimal is the best word here since we arbitrarily fixed a value of Δt. Also, there is the technical problem that Gurobi might not have found the true optimal.
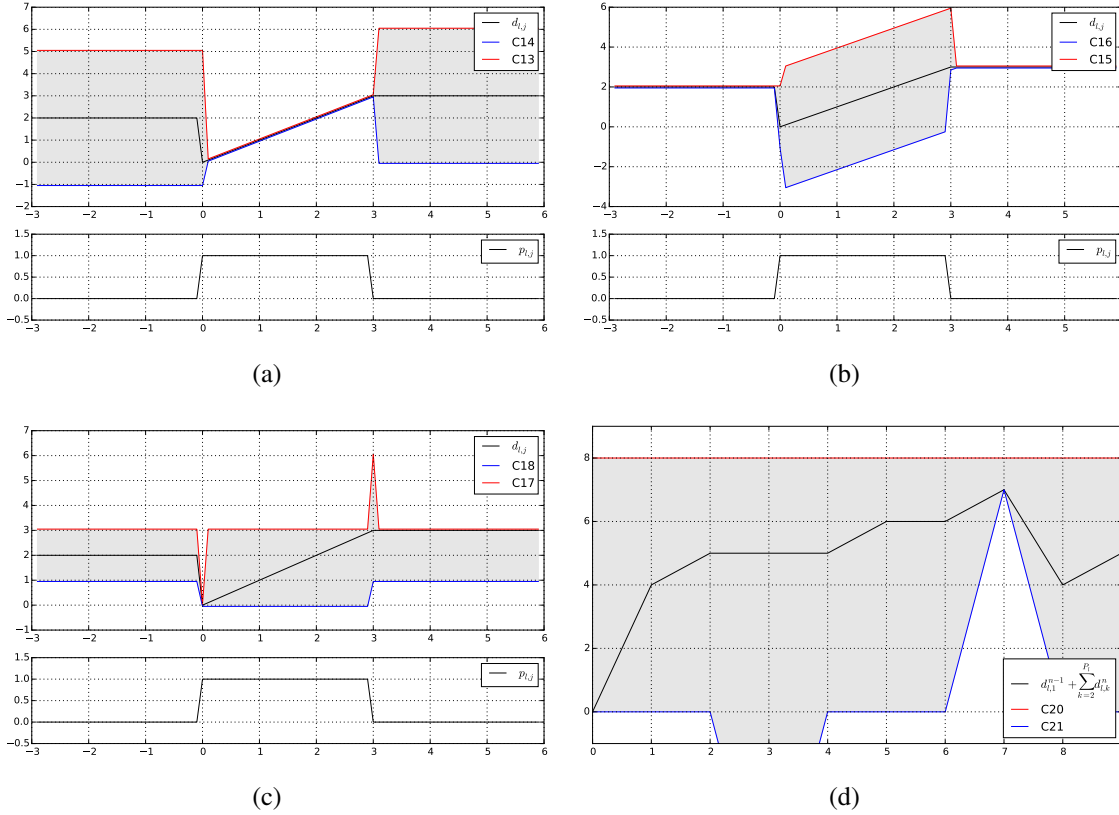
FIGURE 4 **An example showing the phase and cycle time constraint envelopes. In (a), (b) and (c), $\Phi_{\ell,k}^{\min} = 1$ and $\Phi_{\ell,k}^{\max} = 3$, the duration of the previous activation was 2 and the duration of the current activation is 3. In (d), the total cycle time is 7 with $\Psi_{\ell}^{\min} = 7$, $\Psi_{\ell}^{\max} = 8$**

1 requires less time intervals (i.e., smaller N) than the homogeneous approach to converge to the
2 optimal solution. In the remainder of this section, we present the traffic networks considered in the
3 experiments, our methodology, and the results.

4 **Networks**
5 We consider three networks of increasing complexity (Figure 6): an avenue crossed by three side
6 streets; a 2-by-3 grid; and a 3-by-3 grid with a diagonal avenue. The queues receiving cars from
7 outside of the network are marked in Figure 6 and we refer to them as input queues. The maximum
8 capacity (Q_i) is 60 cars for non-input queues and infinity for input queues to prevent interruption
9 of the input demand due to spill back from the stop line. The traversal time of each queue i (T_i^{prop})
10 is set at 9s (a distance of about 100m with a free flow speed of 50km/h). Flows are defined from
11 the head of each queue i into the tail of the next queue j; there is no turning traffic ($\mathrm{Pr}_{i,j} = 1$),
12 and the maximum flow rate between queues, $F_{i,j}$, is set at 5 cars/s. All traffic lights have two
13 phases, north-south and east-west, and lights 2, 4 and 6 of network 3 have the additional northeast-
14 southwest phase to control the diagonal avenue. For networks 1 and 2, $\Phi_{\ell,k}^{\min}$ is 1s, $\Phi_{\ell,k}^{\max}$ is 3s, $\Psi_{\ell}^{\min}$
15 is 2s, and $\Psi_{\ell}^{\max}$ is 6s, for all traffic light ℓ and phase k. For network 3, $\Phi_{\ell,k}^{\min}$ is 1s and $\Phi_{\ell,k}^{\max}$ is 6s
16 for all ℓ and k; and $\Psi_{\ell}^{\min}$ is 2s and $\Psi_{\ell}^{\max}$ is 12s for all lights ℓ except for lights 2, 4 and 6 in which

FIGURE 5 Receding horizon control. For this figure, the problem horizon T **is 40s. The major frames are discretized in 12 time intervals (**$\mathrm{N} = 12$**) and they span 15s and 30s for homogeneous and non-homogeneous discretizations, respectively.**

1 $\Psi_\ell^{\min}$ is 3s and $\Psi_\ell^{\max}$ is 18s.

2 **Experimental Methodology**
3 For each network, a constant background level traffic is injected in the network in the first 55s to
4 allow the solver to settle on a stable policy. Then a spike in demand is introduced in the queues
5 marked as ♠ (Figure 6) from time 55s to 70s to trigger a policy change. From time 70s to 85s,
6 the demand is returned to the background level, and then reduced to zero for all input queues. We
7 extend the problem horizon T until all cars have left the network. By clearing the network, we can
8 easily measure the total travel time for all the traffic as the area between the cumulative arrival and
9 departure curves measured at the boundaries of the network.[11] The background level for the input
10 queues are 1, 4 and 2 cars/s for queues marked as ◇, ♣ and ♠ (Figure 6), respectively; and during
11 the high demand period, the queues ♠ receive 4 cars/s.
12   For both homogeneous and non-homogeneous intervals, we use the MILP QTM formula-
13 tion (Section 3) in a receding horizon manner: a control plan is computed for a pre-defined horizon
14 (smaller than T) and only a prefix of this plan is executed before generating a new control plan.
15 Figure 5 depicts our receding horizon approach and we refer to the planning horizon as a major
16 frame and its executable prefix as a minor frame. Notice that, while the plan for a minor frame is
17 being executed, we can start computing the solution for the next major frame based on a forecast
18 model.[12]
19   To perform a fair comparison between the homogeneous and non-homogeneous discretiza-
20 tions, we fix the size of all minor frames to 10s and force it to be discretized in homogeneous
21 intervals of 0.25s. For the homogeneous experiments, Δt is kept at 0.25s throughout the major
22 frame; therefore, given N, the major frame size equals $\mathrm{N}/4$ seconds for the homogeneous ap-
23 proach. For the non-homogeneous experiments, Δt linearly increases from 0.25s at the end of
24 the minor frame to 1.0s at the end of the major frame; therefore, the major frame size used by
25 the non-homogeneous approach is $10.375 + 0.625(\mathrm{N} - 40)$ seconds for a given $\mathrm{N} > 40$. Once
26 we have generated a series of minor frames, we concatenate them into a single plan and simulate
27 the flow through the network using the QTM LP formulation with a fixed (homogeneous) Δt of

---

[11]FWT: is this explanation of how to compute the total travel time still necessary?
[12]FWT: not sure if we should mention this.

(a)

(b)

(c)

(d)
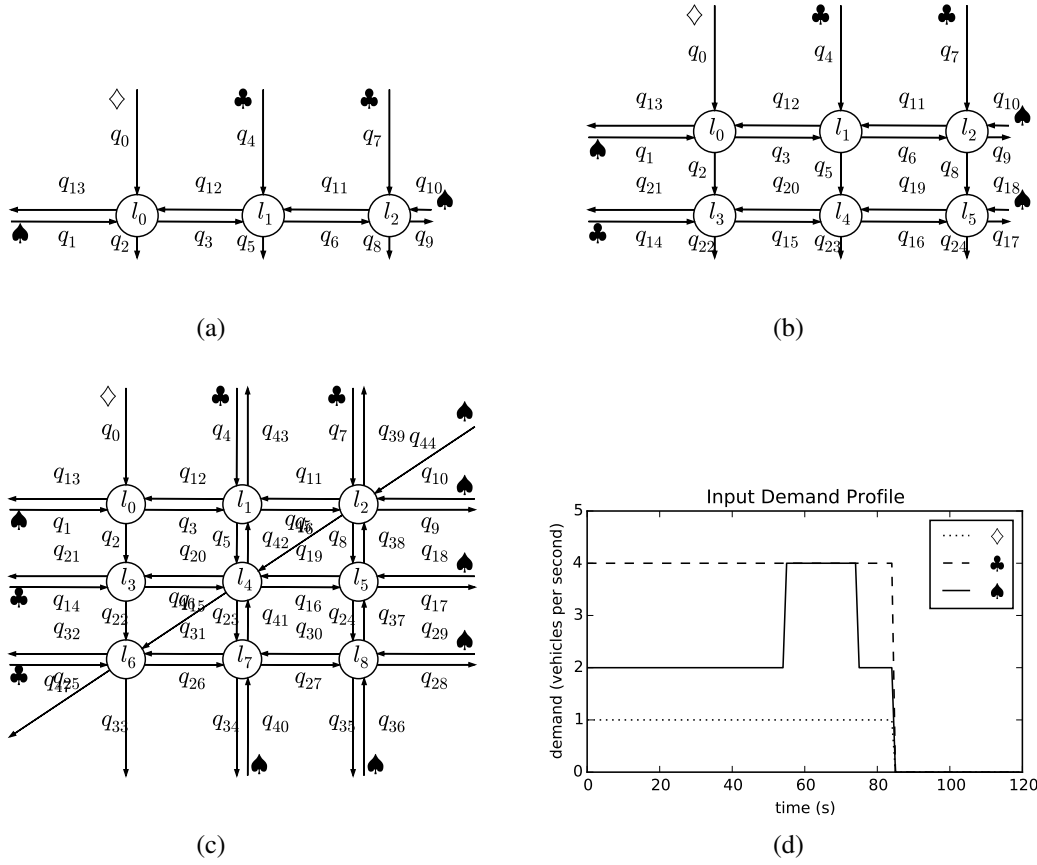
FIGURE 6 Networks used to evaluate the QTM performance. Iain: please, mark the input queues.

1 0.25s. [13] We also compare both receding horizon approaches against the optimal solution obtained
2 by computing a single control plan for the entire control horizon (i.e., $[0, \mathrm{T}]$) using a fixed Δt of
3 0.25s.
4   For all our experiments, we used Gurobi$^{\mathrm{TM}}$ as MILP solver with 12 threads on a 3.1GHz
5 AMD Opteron$^{\mathrm{TM}}$ 4334 processor with 12 cores. We limit MIP gap accuracy to 0.1% and the time
6 cutoff for solving a major frame to 3000s for the receding horizon approaches and unbounded for
7 the optimal plan. All our results are averaged over five runs to account for Gubori's stochastic
8 strategies.

9 **Results**
10 Figures 7(a), 7(c) and 7(e) show, for each network, the increase in the total travel time w.r.t. the
11 optimal solution as a function of N. As we hypothesized, the non-homogeneous discretization
12 requires less time intervals to converge. This is important because the size of the MILP, including
13 the number of binary variables, scales linearly with N; therefore, the non-homogeneous approach
14 can scale up better than the homogeneous one (e.g., Figure 7(e)).
15   The distribution of the total delay observed by each car while traversing the network is

_____

[13]Do we need to justify why we use the QTM as the simulator over say a micro simulator?

1 shown in Figures 7(b), 7(d) and 7(f). Each group of box plots represents a different value of N:
2 when the non-homogeneous Δt first converges to the optimum solution; when the homogeneous
3 Δt first converges on the optimum solution; and the optimum solution itself. In all networks, the
4 quality of the solution obtained using non-homogeneous Δt is better or equal than using homo-
5 geneous Δt for fixed N in both the total travel time and *fairness*, i.e., smaller third quartile and
6 maximum delay.
7   FWT: In the paragraphs above, we need to address network 2 because it is the exception
8 in both cases: in the end of Figure 7(c), homogeneous is better, and the homogeneous delay in
9 Figure 7(d) is also better.
10   Finally, Figure 8 shows the cumulative arrival and departure curves and the how delay
11 evolves over time for q_1 of network 2. Figure 8(a) shows the comparison at the point where the
12 non-homogeneous Δt first converges and shows that with the longer major frame time of the
13 non-homogeneous Δt, the solver is able to find a coordinated signal policy along the avenue to
14 dissipate the extra traffic that arrives at the 55s point, while the homogeneous Δt with its shorter
15 major frame. Once the homogeneous Δt has converged in Figure 8(b), both solutions are close to
16 the optimum solution which is shown in Figure 8(c).[14]

CONCLUSION

18 In this paper, we showed how to formulate a novel queue transmission model (QTM) model of
19 traffic flow with non-homogeneous time steps as a linear program. We then proceeded to allow the
20 traffic signals to become discrete variables subject to a delay minimizing optimization objective
21 and standard traffic signal constraints leading to a final MILP formulation of traffic signal control.
22 We experimented with this novel QTM-based MILP control in a range of networks and demon-
23 strated that by exploiting the non-homogeneous time steps supported by the QTM, we are able
24 to scale the model up to larger networks whilst maintaining the same quality of a homogeneous
25 solution using more binary variables. Altogether, this work represents a major step forward in the
26 scalability of MILP-based jointly optimized traffic signal control via the use of a non-homogeneous
27 traffic models and thus helps pave the way for fully optimized joint urban traffic signal controllers
28 as an improved successor technology to existing signal control methods.

REFERENCES

37 [1] El-Tantawy, S., B. Abdulhai, and H. Abdelgawad, Multiagent reinforcement learning for
38   integrated network of adaptive traffic signal controllers (MARLIN-ATSC): methodology
39   and large-scale application on downtown toronto. *Intelligent Transportation Systems, IEEE*
40   *Transactions on*, Vol. 14, No. 3, 2013, pp. 1140–1150.

---

[14]FWT: although Figure 8 is a nice illustration of how homogeneous and non-homogeneous differ, it is currently not backing up any of our claims.
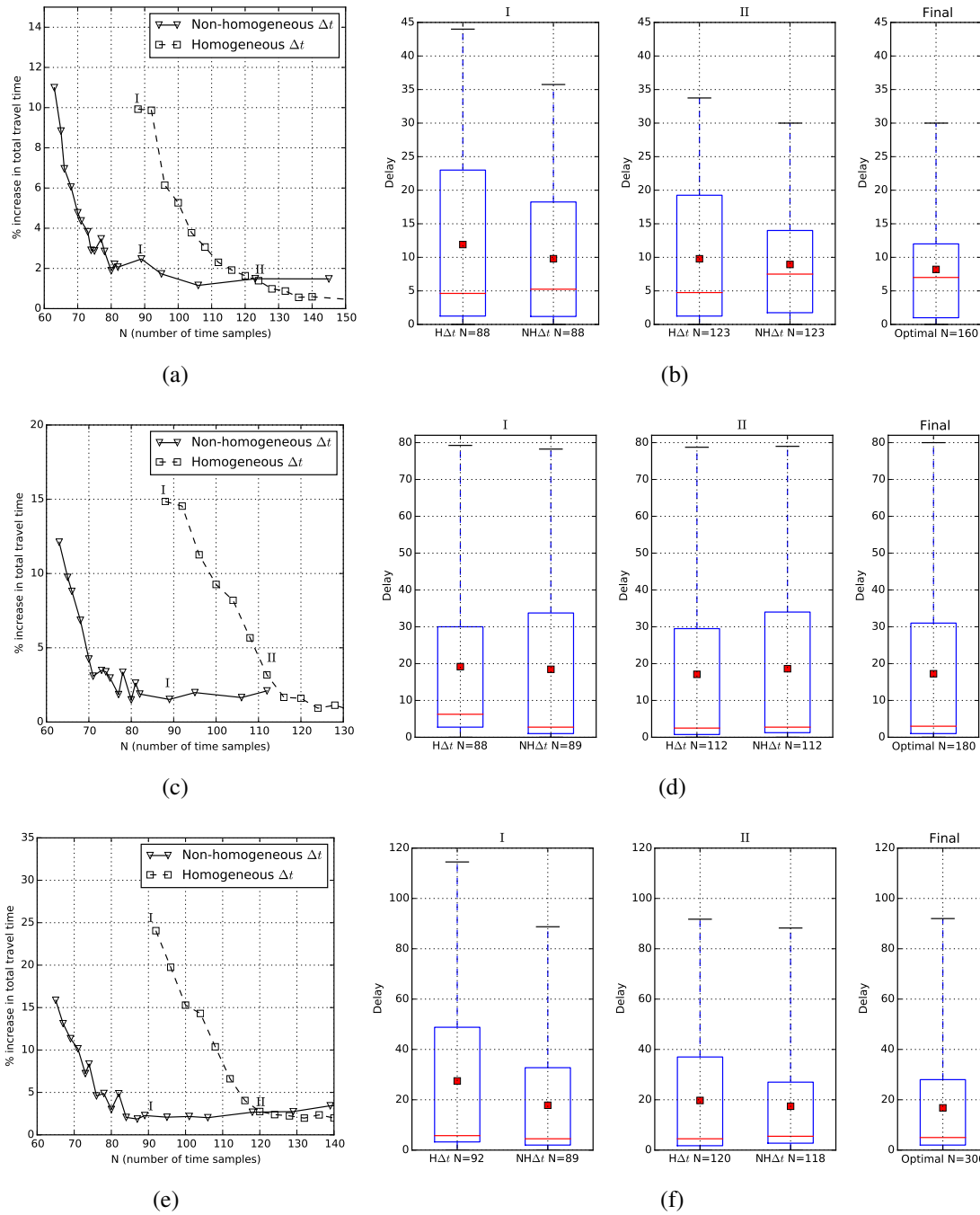
FIGURE 7 Increase in the total travel time w.r.t. the optimal solution as a function of N **(Figures a, c, and e) and distribution of the total delay of each car for different values of** N **(Figures b, d, and f). The mean of the total delay is presented as a red square in box plots. Plots in the** i**-th row correspond to the results for the** i**-th network in Figure 6.**

1   [2] Sims, A. G. and K. W. Dobinson, SCAT–The Sydney co-ordinated adaptive traffic system:
2   Philosophy and benefits. *IEEE Transactions on Vehicular Technology*, Vol. 29, 1980.
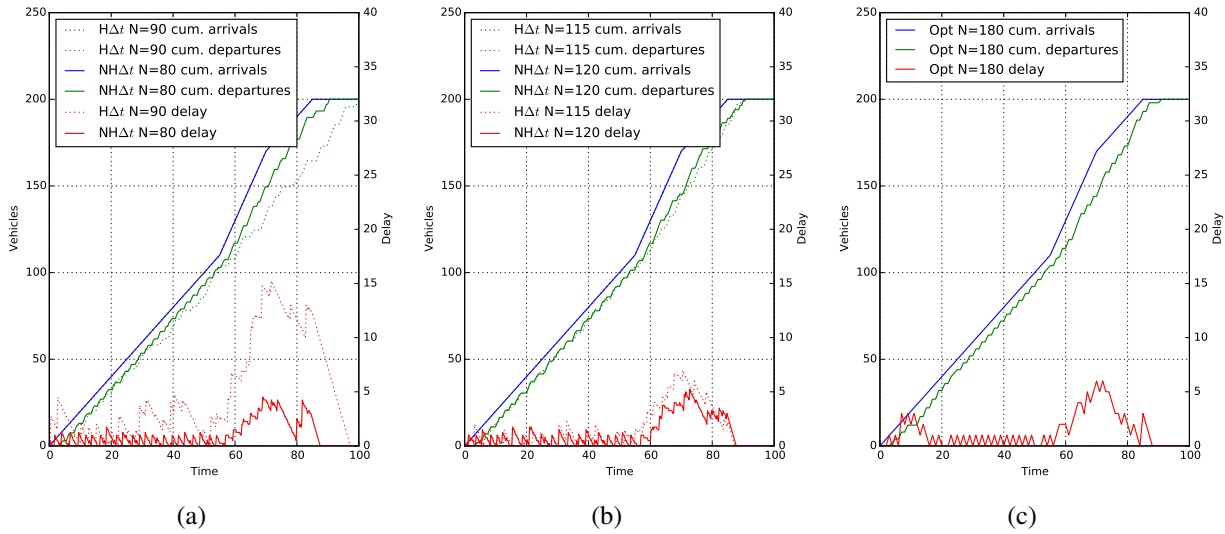
FIGURE 8 Cumulative arrival and departure curves and delay for queue 1 in the 2-by-3 network (Figure 6(b). The value of N in plots (a) and (b) corresponds, respectively, to the convergence point of the non-homogeneous and homogeneous approaches (Figure 7(c)). (c) presents the same curves for the optimal solution.

[3] Hunt, P. B., D. I. Robertson, R. D. Bretherton, and R. I. Winton, *SCOOT–A traffic responsive method of coordinating signals*. Transportation Road Research Lab, Crowthorne, U.K., 1981.

[4] Gartner, N., J. D. Little, and H. Gabbay, *Optimization of traffic signal settings in networks by mixed-integer linear programming*. DTIC Document, 1974.

[5] Gartner, N. H. and C. Stamatiadis, Arterial-based control of traffic flow in urban grid networks. *Mathematical and computer modelling*, Vol. 35, No. 5, 2002, pp. 657–671.

[6] Lo, H. K., A novel traffic signal control formulation. *Transportation Research Part A: Policy and Practice*, Vol. 33, No. 6, 1998, pp. 433–448.

[7] He, Q., K. L. Head, and J. Ding, PAMSCOD: Platoon-based Arterial Multi-modal Signal Control with Online Data. *Procedia-Social and Behavioral Sciences*, Vol. 17, 2011, pp. 462–489.

[8] Lin, W.-H. and C. Wang, An enhanced 0-1 mixed-integer LP formulation for traffic signal control. *Intelligent Transportation Systems, IEEE Transactions on*, Vol. 5, No. 4, 2004, pp. 238–245.

[9] Han, K., T. L. Friesz, and T. Yao, A link-based mixed integer LP approach for adaptive traffic signal control. *arXiv preprint arXiv:1211.4625*, 2012.

[10] Lo, H. K., E. Chang, and Y. C. Chan, Dynamic network traffic control. *Transportation Research Part A: Policy and Practice*, Vol. 35, No. 8, 1999, pp. 721–744.

[11] He, Q., W.-H. Lin, H. Liu, and K. L. Head, Heuristic algorithms to solve 0–1 mixed integer LP formulations for traffic signal control problems. In *Service Operations and Logistics and Informatics (SOLI), 2010 IEEE International Conference on*, IEEE, 2010, pp. 118–124.

[12] Smith, S., G. Barlow, X.-F. Xie, and Z. Rubinstein, SURTRAC: Scalable Urban Traffic Control. In *Transportation Research Board 92nd Annual Meeting Compendium of Papers*, Transportation Research Board, 2013.

[13] Daganzo, C. F., The cell transmission model: A dynamic representation of highway traffic consistent with the hydrodynamic theory. *Transportation Research Part B: Methodological*, Vol. 28, No. 4, 1994, pp. 269–287.

[14] Daganzo, C. F., The cell transmission model, part II: network traffic. *Transportation Research Part B: Methodological*, Vol. 29, No. 2, 1995, pp. 79–93.

[15] Xiaojian, H., W. Wei, and H. Sheng, Urban traffic flow prediction with variable cell transmission model. *Journal of Transportation Systems Engineering and Information Technology*, Vol. 10, No. 4, 2010, pp. 73–78.

[16] Sumalee, A., R. Zhong, T. Pan, and W. Szeto, Stochastic cell transmission model (SCTM): A stochastic dynamic traffic model for traffic state surveillance and assignment. *Transportation Research Part B: Methodological*, Vol. 45, No. 3, 2011, pp. 507–533.

[17] Jabari, S. E. and H. X. Liu, A stochastic model of traffic flow: Theoretical foundations. *Transportation Research Part B: Methodological*, Vol. 46, No. 1, 2012, pp. 156–174.

[18] Huang, K. C., *Traffic Simulation Model for Urban Networks: CTM-URBAN*. Ph.D. thesis, Concordia University, 2011.

[19] Muralidharan, A., G. Dervisoglu, and R. Horowitz, Freeway traffic flow simulation using the link node cell transmission model. In *American Control Conference, 2009. ACC'09.*, IEEE, 2009, pp. 2916–2921.

[20] Gomes, G. and R. Horowitz, Optimal freeway ramp metering using the asymmetric cell transmission model. *Transportation Research Part C: Emerging Technologies*, Vol. 14, No. 4, 2006, pp. 244–262.

[21] Kim, Y., *Online traffic flow model applying dynamic flow-density relation*. Int. At. Energy Agency, 2002.

[22] Lu, S., S. Dai, and X. Liu, A discrete traffic kinetic model–integrating the lagged cell transmission and continuous traffic kinetic models. *Transportation Research Part C: Emerging Technologies*, Vol. 19, No. 2, 2011, pp. 196–205.

[23] Alecsandru, C., A. Quddus, K. C. Huang, B. Rouhieh, A. R. Khan, and Q. Zeng, An assessment of the cell-transmission traffic flow paradigm: Development and applications. In *Transportation Research Board 90th Annual Meeting*, 2011, 11-1152.